Dancing between the devil and deep blue sea: the stabilizing effect of enemy-free and victimless sinks

Sebastian J. Schreiber, Romuald N. Lipcius, Rochelle D. Seitz and W. Chris Long

Theoretical and empirical studies have shown that enemy-victim interactions in spatially homogenous environments can exhibit diverging oscillations which result in the extinction of one or both species. For enemy-victim models with overlapping generations, we investigate the dynamical implications of spatial heterogeneity created by enemy-free sinks or victimless sinks. An enemy-free sink is a behavioral, physiological or ecological state that reduces or eliminates the victim's vulnerability to the enemy but cannot sustain the victim population. For victims that move in an ideal-free manner, we prove that the inclusion of an enemy-free sink shifts the population dynamics from diverging oscillations to stable oscillations. During these stable oscillations, the victim disperses in an oscillatory manner between the enemy-free sink and the enemy-occupied patch. Enemy-free sinks with lower mortality rates exhibit oscillations with smaller amplitudes and longer periods. A victimless sink, on the other hand, is a behavioral, physiological or ecological state in which the enemy has limited (or no) access to its victims. For enemies that move in an ideal-free manner, we prove that victimless sinks also stabilize diverging oscillations. Simulations suggest that suboptimal behavior due to information gathering or learning limitations amplify oscillations for systems with enemy-free sinks and dampen oscillations for systems with victimless sinks. These results illustrate that the coupling of a sink created by unstable enemy-victim interactions and a sink created by unsuitable environmental conditions can result in population persistence at the landscape level.

S. J. Schreiber, Dept of Mathematics and Inst. for Integrative Bird Behavior Studies, The College of William and Mary, Williamsburg, VA 23187-8795, USA (sjschr@wm.edu). – R. N. Lipcius, R. D. Seitz and W. C. Long, Virginia Inst. of Marine Science, The College of William and Mary, Gloucester Point, VA 23062, USA.

Introduction

Most species live in heterogenous landscapes and are either victims (e.g. prey, hosts) or enemies (e.g. pathogens, predators, parasitoids) of other species. Landscape heterogeneity often results in spatial variability in population birth and death rates and can partition the landscape into a mosaic of source and sink habitats (Holt 1985, 1997, Pulliam 1988, Dias 1996). In source habitats, populations persist as birth rates exceed death rates. In sink habitats, death rates exceed birth rates.

Even though populations constrained to sink habitats can not persist without immigration of recruits from sources, the presence or absence of sinks can affect victim-enemy interactions. Passive dispersal of an enemy between a source habitat and a sink habitat (e.g. a habitat without any victims) can stabilize an otherwise unstable enemy-victim equilibrium and can increase the equilibrium abundance of the enemy (Holt 1985). At this equilibrium, the per-capita fitness of the enemy is greater in the source. Since individuals would increase their fitness by remaining in the source, this equilibrium is

evolutionarily unstable. So, why do sink populations exist?

Holt (1997) proposed two mechanisms resulting in evolutionarily stable sink populations. First, organisms may be neither ideal nor free. Constraints on dispersal, learning, or information gathering may prevent organisms from distributing themselves in an ideal-free manner (van Baalen and Sabelis 1993, Bernstein et al. 1999, Bolker et al. 2003). Second, non-equilibrium population dynamics may result in moments when the fitness in the sink exceeds the fitness in the source. In these instances, it is advantageous for individuals to move from the source to the sink. While Holt (1997) only explored this latter possibility for single species dynamics, it is also particularly germane for enemy–victim interactions that can generate oscillatory dynamics (Huffaker 1958, Lukinbill 1973, Hassell 1978). In this article, we analyze three models of enemy-victim interactions to determine when oscillatory dynamics coupled with a sink result in evolutionarily stable and ecologically persistent sink populations. Our study begins with a well-known model representing enemy-victim interactions in a homogenous environment (Murdoch and Oaten 1975, Holt 1985). This model is the foundation upon which the remaining models are built and is proven to exhibit a dynamic dichotomy; either both populations grow exponentially or the populations exhibit unbounded oscillations. In the former case, the habitat can be viewed as a source for both populations. In the latter case, demographic stochasticity will result in the extinction of one or both species, and the habitat can be classified as a sink for one or both species.

Our study continues with the inclusion of an enemy-free sink, which is defined as a behavioral, physiological or ecological state that reduces or eliminates the victim's vulnerability to the enemy (Jeffries and Lawton 1984) but cannot sustain the victim population. Enemy-free zones have been observed in many ecosystems. For example, abalones evade severe sea otter predation by residing in crevices that allow limited access by predators (Hines and Pearse 1982). Snails avoid sea star predation by residence on kelp plants and off the sea bottom where sea stars forage (Watanabe 1984). In a terrestrial example, predation by the least weasel can decimate field vole populations in optimal field and meadow habitats, but the predator's hunting efficiency is low on voles in sub-optimal bog habitats. Surviving voles in the sub-optimal habitat (i.e. enemy-free sink) can subsequently re-colonize field and meadow populations, thus stabilizing the population (Ylönen et al. 2003). Furthermore, in a meta-analysis, Denno and Peterson (2000) demonstrate that highly mobile planthopper insects that can avert predators and move to presumably lower-quality habitats have more stable populations than other less-mobile planthopper species. Whether enemy-free zones are sinks depends on the characteristics of the habitat. Enemy-free sinks are, however, likely to be common in ecosystems where anthropogenic stress (e.g. eutrophication, overfishing, habitat degradation, hypoxia) is severe (Jackson et al. 2001). For example, hypoxic environments are lethal to yellow perch, but not to their prey, fathead minnows, and, thus, may be enemy-free sinks (Robb and Abrahams 2002). In our second model, we analyze enemy-victim dynamics with victim movement between the enemy-free sink and the enemy-occupied sink. As such, the victims must move "between the devil and the deep blue sea" (Lawton and McNeill 1979).

Our third model includes a victimless sink, which is a behavioral, physiological or ecological state where the enemy has limited (or no) access to its victims. Victimless sinks can arise when enemy species go into a dormant state at low victim densities. For example, when *Paramecium* densities are too low, the protist predator *Didinium* encysts by producing a cocoon made of clear material that hardens into a thick wall. When *Paramecium* densities increase, *Didinium* excysts and resumes feeding on *Paramecium*. Similarly, some species of copepods cease feeding at low prey densities (Porter et al. 1983). In a terrestrial example of a victimless sink, coyotes in low-quality forest habitats in Quebec cease feeding on small animals in favor of berriesduring the summer, whereas their counterparts in higher-quality rural habitats feed on small animals year round. The coyotes in the sub-optimal summer habitats tend to be lighter and shorter than the coyotes in optimal habitats (Tremblay et al. 1998). In our third model, we analyze the ecological implications of the enemy moving between the victimless sink and the victim-occupied sink.

Our work is related to previous modeling studies on enemy–victim dynamics (Goh 1980, Holt 1984, 1985, McNair 1986, 1987, Křivan 1997, 1998, van Baalen and Sabelis 1999, Bernstein et al. 1999, Schreiber et al. 2000). Goh (1980) studied enemy-victim dynamics in which the victim moves diffusively between an enemy-free patch and an enemy-occupied patch. He found that the inclusion of the enemy-free patch could stabilize the enemy-victim equilibrium. This stabilizing effect of a victim refuge, however, may be disrupted if the victim dynamics in the refuge are unstable (McNair 1987). Holt (1984, 1985) found that diffusive movement of an enemy between a victimless sink and a victim-occupied sink can stabilize the enemy-victim equilibrium. In contrast to these predictions about diffusive movement, Křivan (1997, 1998) showed that for Lotka-Volterra enemy-victim systems with and without victim refuges, ideal-free movement between patches could stabilize neutrally stable dynamics. Similarly, van Baalen and Sabelis (1999) studied Nicholson-Bailey host–parasitoid models which have inherently unstable dynamics. The inclusion of ideal-free movement between (but not within) generations was shown via simulations to stabilize the dynamics

about non-equilibrium attractors when there were low quality (e.g. sinks) patches for the hosts. Finally, Bernstein et al. (1999) found that for continuous-time enemy–victim systems without refuges or sinks, ideal-free movement of the enemy had no effect on stability of the equilibrium provided that all species dispersed quickly. However, at lower migration rates, suboptimal movement of the enemy could stabilize the enemy-victim equilibrium.

In contrast to these studies, we consider enemy–victim interactions that are inherently unstable, include enemy or victim refuges, and allow for a continuum of dispersal strategies from passive dispersal to ideal-free movement. In particular, we prove that adaptive habitat choice promotes oscillatory coexistence in the presence of enemy-free sinks or victimless sinks. Moreover, we numerically investigate how non-adaptive habitat choice either due to limited dispersal abilities or limited knowledge about the environment amplify or dampen oscillations.

The models

Our models revolve around a dynamically unstable enemy–victim interaction in a habitat for which the victim exhibits exponential growth in the absence of the enemy. Let N and P be the victim and enemy densities, respectively, r the intrinsic rate of growth of the victim, $Ng(N)$ the functional response of the enemy, and $h(N)$ the numerical response of the enemy. These assumptions lead to the following well-known model (Murdoch and Oaten 1975, May 1981, Holt 1985)

$$\frac{dN}{dt} = r\,N - P\,N\,g(N)$$

$$\frac{dP}{dt} = P\,h(N) \tag{1}$$

Since increasing victim densities increases the rate at which victims are consumed and increases the enemy's growth rate, the functional and numerical responses of the enemy are assumed to increase with N. The function $g(N)$ is proportional to the fraction of actively searching predators and is assumed to be a decreasing function of N (i.e. predators satiate or exhibit handling times). Finally, as enemies require victims for sustenance, the per-capita growth rate $h(0)$ of the enemy in the absence of victims is assumed to be negative.

To account for movement of individuals between two states (e.g. an enemy-free state and enemy-occupied state), we assume the per-capita movement rate from one state, call it state 1, to the other, call it state 2, depends on the difference between the per-capita growth rates $r_1 - r_2$ in the two states:

$$\frac{d}{1 + \exp(\gamma(r_1 - r_2))}$$

where d is the maximum per-capita movement rate and γ determines how quickly individuals respond to differences in the per-capita growth rates. Roughly, the higher the value of γ, the more ideally individuals respond to differences in per-capita growth rates. In particular, $\gamma = 0$ corresponds to passive movement and $\gamma \uparrow \infty$ corresponds to individuals moving at a maximal rate to the state with the higher per-capita growth rate. When $\gamma \uparrow \infty$ and $d \uparrow \infty$, individuals exhibit ideal-free movement, an evolutionarily stable strategy for our models.

To account for an enemy-free sink, we assume the victim's per-capita growth rate r_2 is negative in this state. If N_1 and N_2 denote the densities of the prey outside and inside the enemy-free sink, respectively, then the enemy-victim dynamics become

$$\frac{dN_1}{dt} = rN_1 - N_1 Pg(N_1) - \frac{dN_1}{1 + \exp(\gamma(r - Pg(N_1) - r_2))}$$

$$+ \frac{dN_2}{1 + \exp(\gamma(r_2 - r + Pg(N_1)))}$$

$$\frac{dN_2}{dt} = r_2 N_2 + \frac{dN_1}{1 + \exp(\gamma(r - Pg(N_1) - r_2))}$$

$$- \frac{dN_2}{1 + \exp(\gamma(r_2 - r + Pg(N_1)))}$$

$$\frac{dP}{dt} = P\,h(N_1) \tag{2}$$

An alternative to augmenting a homogenous landscape with enemy-free sinks is augmenting it with victimless sinks. Assume the enemy per-capita growth rate r_2 in this victimless sink is negative. If P_1 and P_2 denote the densities of the predator outside and inside the victimless sink, respectively, then the enemy–victim dynamics become

$$\frac{dN}{dt} = rN - NP_1 g(N)$$

$$\frac{dP_1}{dt} = P_1\,h(N_1) - \frac{dP_1}{1 + \exp(\gamma(h(N_1) - r_2))}$$

$$+ \frac{dP_2}{1 + \exp(\gamma(r_2 - h(N_1)))}$$

$$\frac{dP_2}{dt} = r_2 P_2 + \frac{dP_1}{1 + \exp(\gamma(h(N_1) - r_2))}$$

$$- \frac{dP_2}{1 + \exp(\gamma(r_2 - h(N_1)))} \tag{3}$$

For Eq. 2 and 3, we provide a relatively complete analysis in the limiting case of ideal-free movement (i.e. d, γ approach ∞). To understand how non-ideal or

non-free movement affects our results, we perform numerical simulations when the enemy has a Holling type II functional response. More precisely, $N\,g(N) = \frac{aN}{1+aT_hN}$ where a and T_h are the enemy searching efficiency and handling time, and $h(N) = cN\,g(N) - m$ where c and m are the enemy conversion efficiency and per-capita mortality rate, respectively.

Results

Enemy−victim interactions in a homogenous environment

An important quantity for (1) is the "intrinsic" per-capita growth rate ρ of the enemy which corresponds to the enemy's per-capita growth rate when victims are abundant (i.e. $\rho = \lim_{N \to \infty} h(N)$). Throughout this article, we assume that ρ is positive else the enemy has no chance for survival. Under this assumption, this system has a unique equilibrium

$$N^* = h^{-1}(0) \quad P^* = \frac{r}{g(N^*)}$$

at which both populations coexist. This equilibrium is known to be unstable. In Appendix A, we prove that dynamics of (1) come in two flavors:

Enemy−victim sink. The enemy and victim exhibit more and more severe oscillations that result in arbitrarily low and high victim and enemy densities (Fig. 1a, 1b). In the presence of demographic stochasticity, these undamped oscillations inevitably result in the extinction of the enemy or both species. Thus, the presence of the enemy transforms a source habitat for the victim to a sink habitat for at least one of the species.
Enemy−victim source. After some initial oscillations, the enemy and victim numbers grow at an exponential rate (Fig. 1c, 1d).

In the next three sections, we focus on how the addition of enemy-free sinks or victimless sinks affects the dynamics of enemy−victim sinks.

Inclusion of enemy−free sinks

If the victims have ideal-free access to the enemy-free sink (i.e. γ, d approach ∞ in (2)), then the enemy−victim dynamics simplify to

$$\frac{dN}{dt} = \begin{cases} r_2\,N & \text{if } r_2 > r - P\,g(N) \\ r\,N - P\,N\,g(N) & \text{if } r_2 < r - P\,g(N) \end{cases}$$

$$\frac{dP}{dt} = \begin{cases} P\,h(0) & \text{if } r_2 > r - P\,g(N) \\ P\,h(N) & \text{if } r_2 < r - P\,g(N) \end{cases} \tag{4}$$

Even though these equations are only defined when $r_2 \neq r - P\,g(N)$, the population trajectories of (4) extend naturally to the "switching curve" $P = \frac{r - r_2}{g(N)}$ i.e. the set of enemy−victim densities at which the per-capita growth rate of the victim in both states is negative and equal to r_2. Population trajectories hitting this curve can do one of two things. At points on the switching curve where growth rate vectors $(\frac{dN}{dt}, \frac{dP}{dt})$ on either side point toward the switching curve, population trajectories slide along the switching curve in a uniquely specified way described in Appendix B (Fig. 2a). Alternatively, at points where all growth rate vectors near the switching curve point downward, population trajectories pass through the switching curve (Fig. 2b). When a population trajectory slides down the switching curve (Fig. 2a), the victim spends a fraction α of its time with enemies.

In Appendix B, we prove three results about an enemy-free sink augmenting an enemy−victim sink. First, all non-equilibrium population trajectories of (4) eventually hit the switching curve and converge to a globally attracting periodic population trajectory. Hence, the inclusion of an enemy-free sink strongly dampens and stabilizes the enemy−victim oscillations, ensuring the long-term persistence of both populations (Fig. 3a−b). Second, this periodic population trajectory has one segment along the switching curve during which the victim enters the enemy-free sink (Fig. 3c). Hence, the victims move periodically between the enemies and the enemy-free sink, entering the enemy-free sink when enemy population densities are high and leaving the enemy-free sink when enemy population densities are low. Third, increasing the per-capita growth rate r_2 of the victim in the enemy-free sink brings the switching curve closer to the victim nullcline and thereby decreases the amplitude of the enemy−victim oscillations. In fact, in the extreme case when the enemy-free sink is of marginal quality for the victim (i.e. $r_2 = 0$), the enemy−victim equilibrium becomes globally stable.

When the victims do not exhibit ideal-free movement, the inclusion of an enemy-free sink may no longer stabilize the enemy−victim interaction. Freely moving victims that respond slowly to differences in per-capita growth rates (i.e. γ small and d large) generate extreme oscillations that in a more realistic model accounting for demographic stochasticity would lead to rapid extinction of one or both species (Fig. 4a). In contrast, victims that respond more ideally to differences in per-capita growth rates dampen the oscillations (Fig. 4b, 4c). Similarly, higher dispersal rates result in higher minimum population densities and, consequently, a lower risk of extinction (Fig. 4d). An interesting exception to this trend is victims that effectively disperse passively (i.e. γ small), in
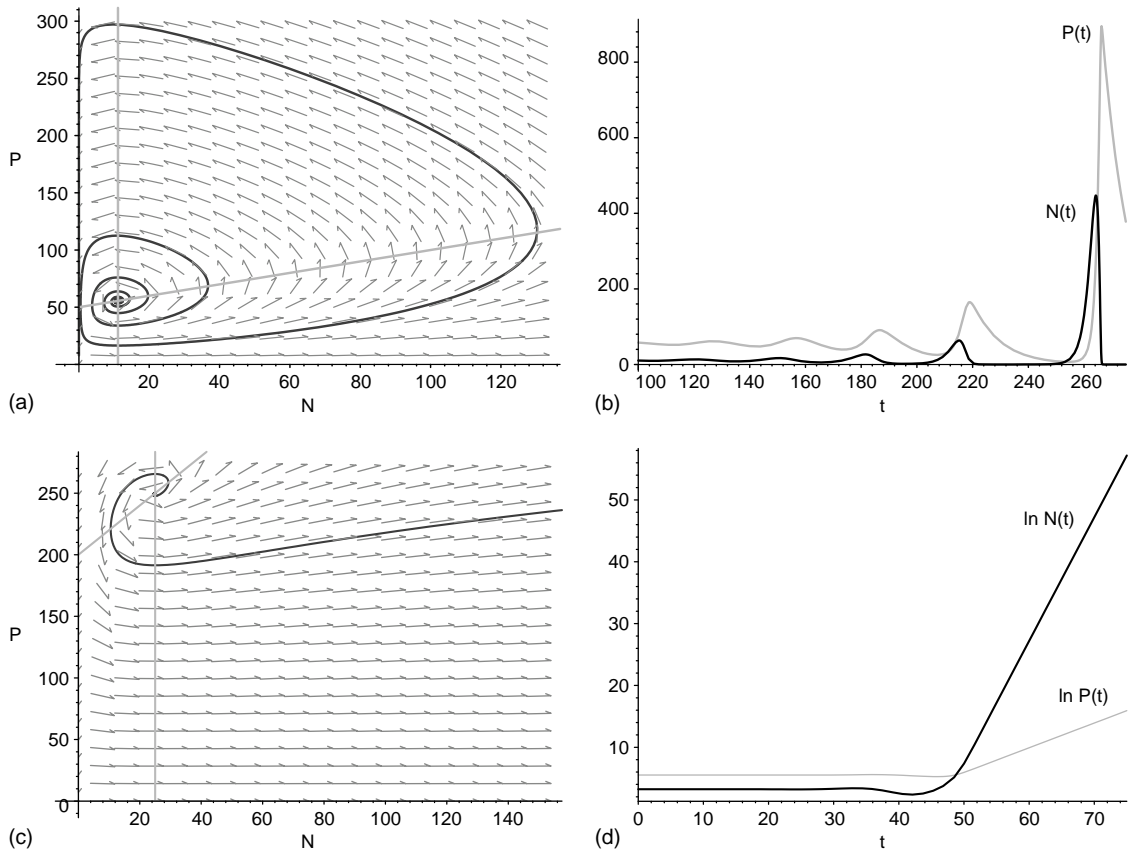
Fig. 1. Two types of dynamics for homogenous enemy-victim interactions as modelled by (1). In (a) and (b), the enemy over-exploits the victim. In (c) and (d), both populations exhibit exponential growth. (a) and (c) are phase portraits with arrows representing growth vectors $(\frac{dN}{dt}, \frac{dP}{dt})$, grey lines representing nullclines, and the solid curve a typical population trajectory. In (b), enemy and victim densities of the population trajectory in (a) are plotted against time. In (d), the logarithm of enemy and victim densities of population trajectory in (c) are plotted against time
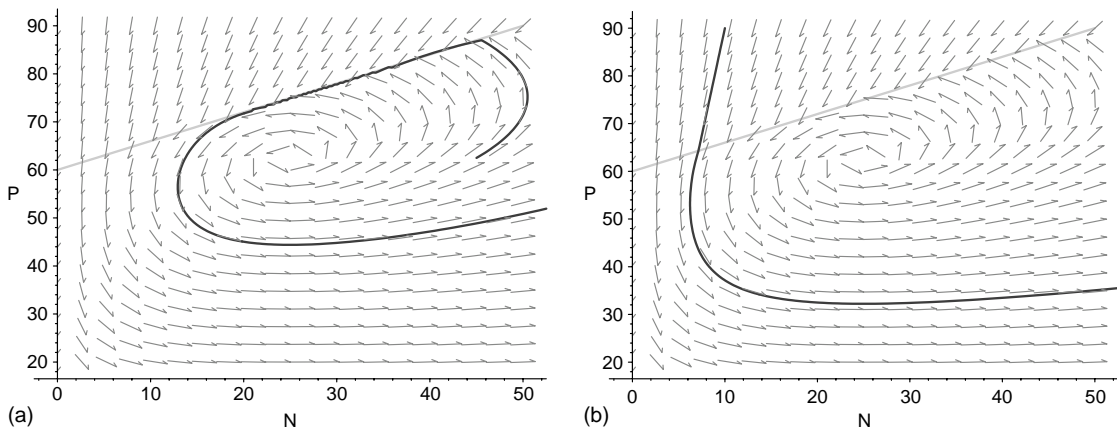
Fig. 2. Two dynamics on the switching curve of (4) with $Ng(N) = \frac{a\,N}{1+T_h a\,N}$ and $h(N) = \theta\,N\,g(N) - m$. The arrows represent growth vectors $(\frac{dN}{dt}, \frac{dP}{dt})$, the solid grey curve represents the switching curve, and the solid black curve represents a population trajectory. In (a), a population trajectory hits and follows the switching curve. In (b), a population trajectory passes through the switching curve.
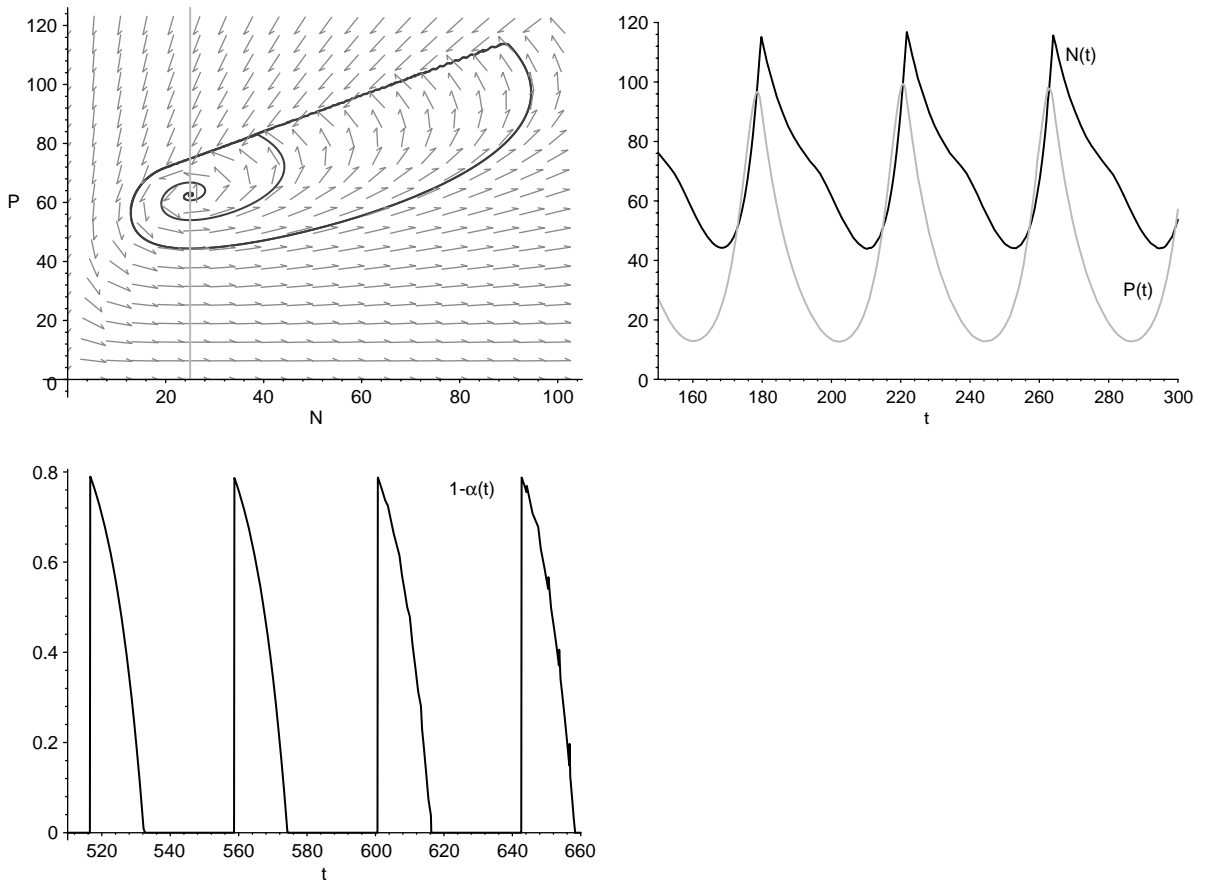
Fig. 3. The dynamics of (4) when $Ng(N) = \frac{a\,N}{1 + T_h a\,N}$ and $h(N) = \theta\,N\,g(N) - m$. In (a) all populations in the victim–enemy phase space approach a unique periodic trajectory. The enemy and total victim densities of this periodic trajectory are plotted against time in (b). In (c), the fraction $1 - \alpha(t)$ of time that the victims spend in the enemy-free sink is plotted against time.

which case the minimum prey density is maximized at intermediate dispersal rates.

Inclusion of victimless sinks

If the enemy has access to victimless sinks and is ideal and free (i.e. γ, d approach ∞ in (3)), then the enemy-victim dynamics simplify to

$$\frac{dN}{dt} = \begin{cases} r\,N & \text{if } r_2 > h(N) \\ r\,N - P\,N\,g(N) & \text{if } r_2 < h(N) \end{cases}$$

$$\frac{dP}{dt} = \begin{cases} r_2\,P & \text{if } r_2 > h(N) \\ P\,h(N) & \text{if } r_2 < h(N) \end{cases} \quad (5)$$

Even though these equations are only defined when $r_2 \neq h(N)$, the population trajectories of (5) naturally extend in a unique way to the victim "switching line" $N = h^{-1}(r_2)$. Population trajectories $(N(t), P(t))$ hitting this switching line can do one of two things depending on whether they hit the switching line above or below the point $(\tilde{N}, \tilde{P}) = (h^{-1}(r_2), \frac{r}{g(h^{-1}(r_2))})$ where the switching line

intersects the victim nullcline. If a population trajectory hits the switching line above this point, then the trajectory slides down the switching line to the point $(\tilde{N}, \tilde{P})$ (Fig. 5a). When this occurs, the enemies spend a fraction α of time with the victims (Appendix C). If a population trajectory hits the switching line below $(\tilde{N}, \tilde{P})$, then the trajectory passes through the switching line (Fig. 5b).

Using arguments similar to those found in Appendix B, we can draw three conclusions. First, whenever a population trajectory $(N(t), P(t))$ initiated at $(\tilde{N}, \tilde{P})$ eventually exhibits a decline in victim numbers, then this solution forms a stable periodic trajectory to (5). In particular, when the populations exhibit unbounded oscillations in the absence of the victimless sink, the inclusion of the victimless sink produces a globally stable periodic motion (Fig. 6a–b). Second, along this periodic motion, the minimum victim density is given by $N = h^{-1}(r_2)$. Consequently, the higher the per-capita growth rate r_2 of the enemy in the victimless sink, the higher the minimum victim density. Third, along this periodic motion, the enemy dances between
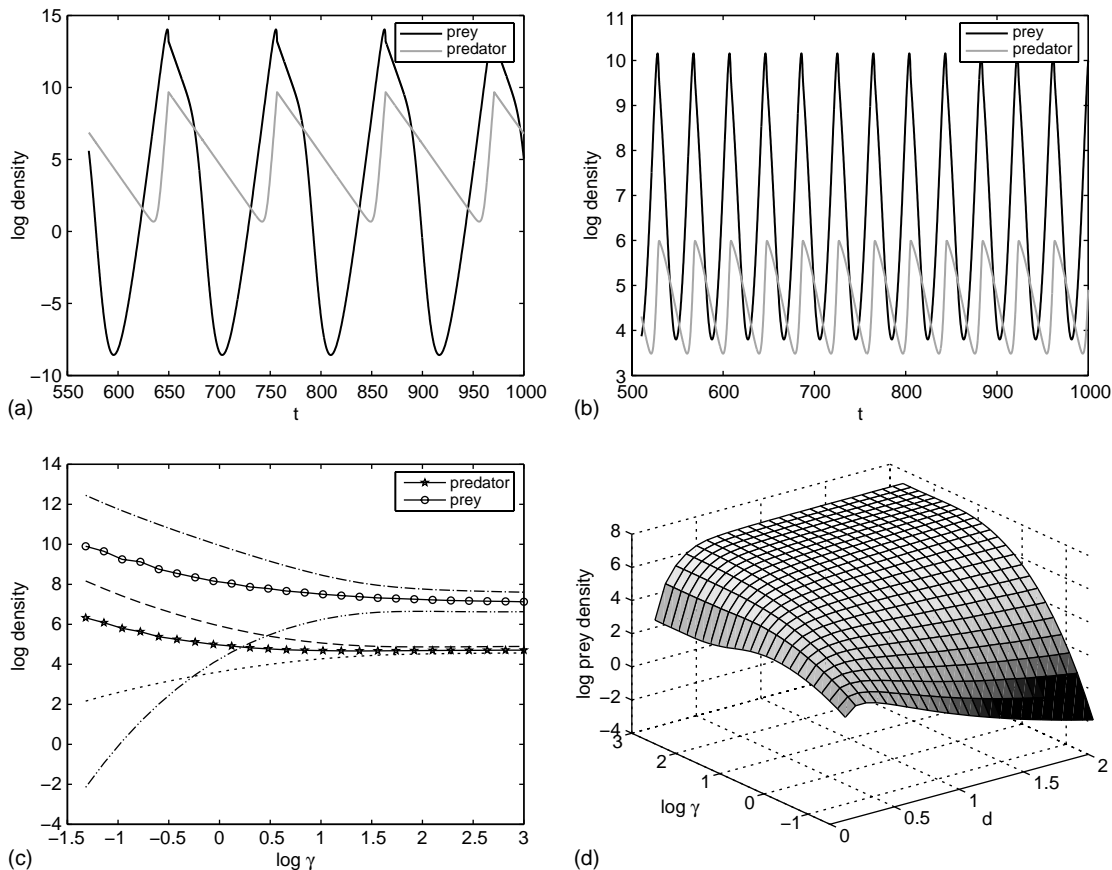
Fig. 4. Population dynamics of (2) with $g(N_1) = \frac{0.001}{1 + 0.001\, N_1} - 0.1$, $r_1 = -0.2$, $r_2 = -0.2$, and $h(N_1) = \frac{0.001}{1 + 0.001\, N_1} - 0.1$. In (a), $d = 2$ and $\gamma = 0.2$. In (b), $d = 2$ and $\gamma = 1$. In (c), $d = 2$ and $\log \gamma$ varies as shown. Simulations are run for 1000 time units and the average (solid lines with circles or stars), minimum (dashed), and maximum (dashed) densities are shown on a log scale for the last 500 time units. In (d), d and $\log \gamma$ vary as shown. Simulations are run for 1000 time steps and the minimum prey density in the last 500 time steps is plotted on a log scale.
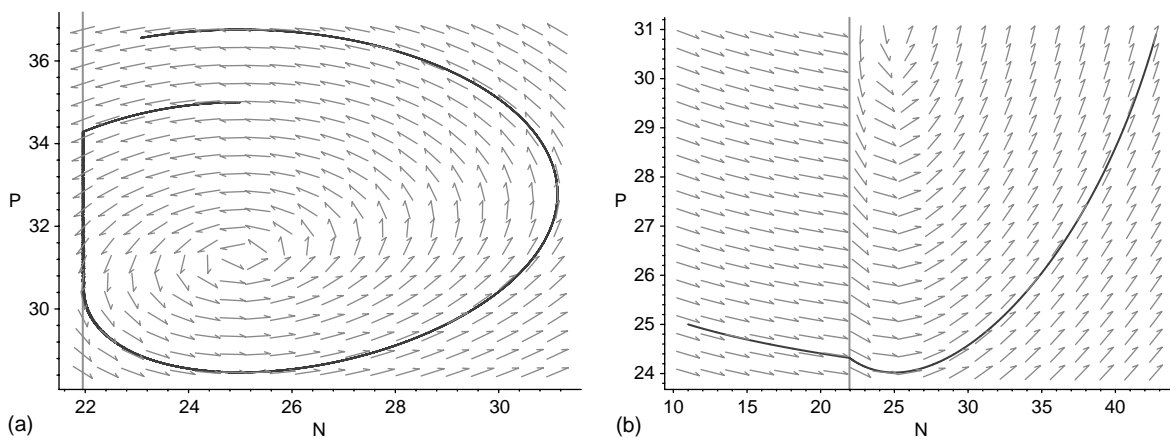
Fig. 5. Crossing the switching line of (5). The arrows represent growth vectors, the grey line is the switching line, and the solid black curve is a population trajectory. In (a), a population trajectory hits the switching line above the point (N, P), slides down the switching line until the point (N, P), and exits to the right of the switching line. In (b), a population trajectory hits and passes through the switching line below the point (N, P).
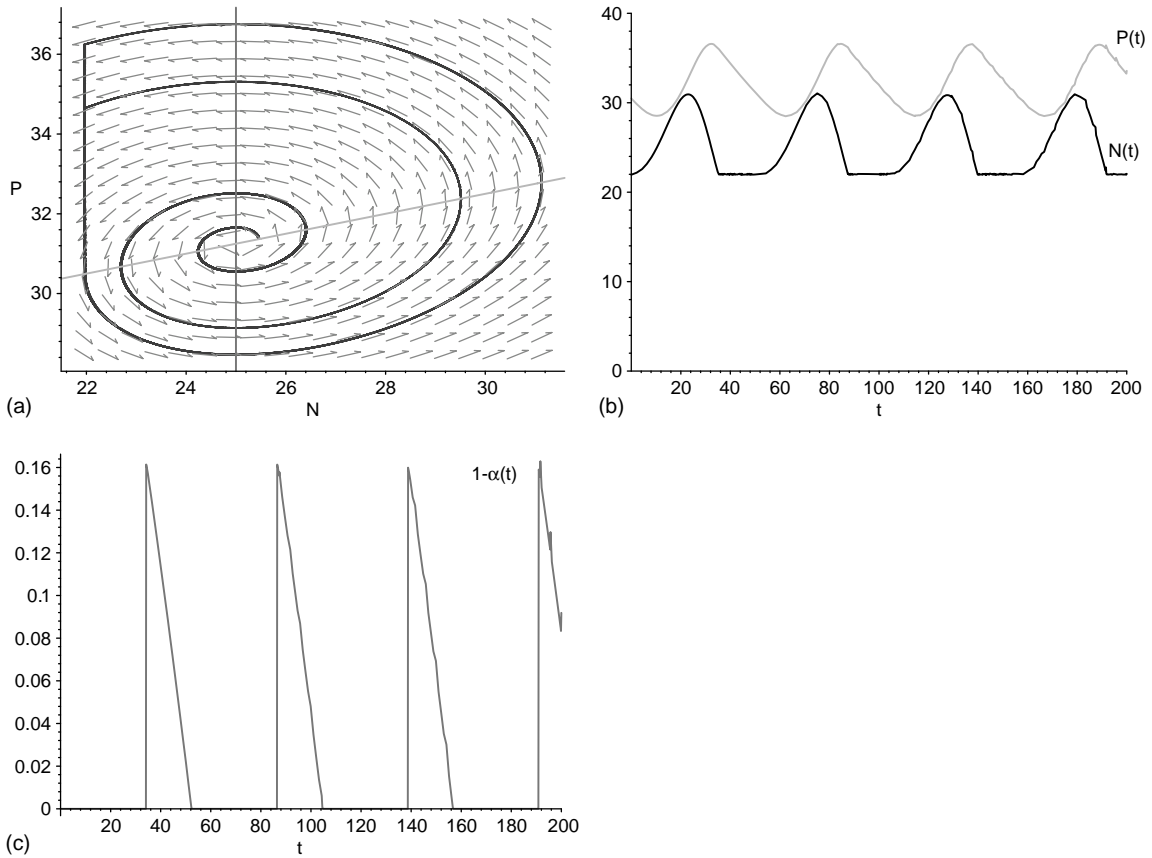
Fig. 6. The dynamics of (5) when enemy-victim interactions generate unbounded oscillations in the absence of the victimless sink. In (a), all solutions in the victim–enemy phase space approach a periodic solution. The enemy and total victim densities of this periodic solution are plotted against time in (b). In (c), the fraction of time spent by the enemy (equivalently, the fraction of enemies) in the sink is plotted against time.

the victims and the victimless sink, entering the victimless sink when the victim density is Ñ and exiting the victimless sink when victim density increases again (Fig. 6c).

In contrast to enemy-free sinks, ideal-free movement of the enemies into victimless sinks can generate oscillations with larger amplitudes than more diffusive movement of enemies (Fig. 7). However, these larger
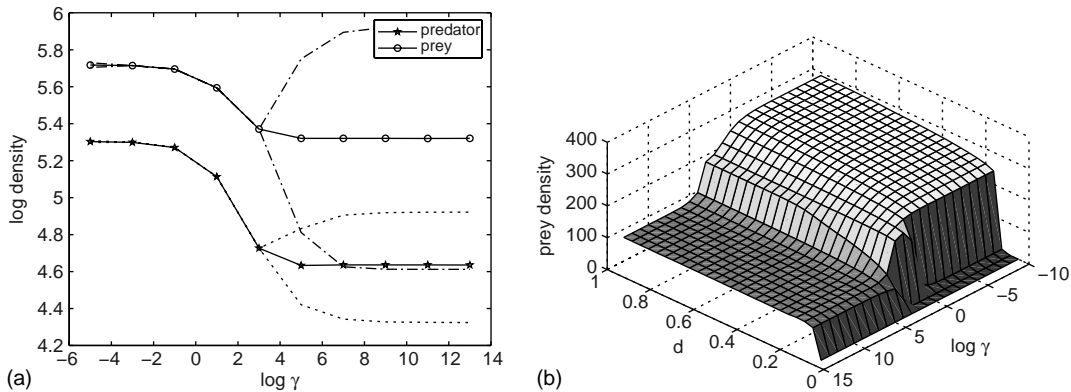
Fig. 7. Population dynamics of (3) with $g(N_1) = \frac{0.01}{1+0.001\,N_1}$ $r_1 = 1$, $r_2 = -0.1$, $h(N_1) = \frac{0.001}{1+0.001\,N_1} - 0.2$. In (a), $d = 4$ and $\log \gamma$ varies as shown. Simulations are run for 1000 time units and the average (solid lines with circles or stars), minimum (dashed), and maximum (dashed) densities are shown on a log scale for the last 500 time units. In (b), d and $\log \gamma$ vary as shown. Simulations are run for 1000 time steps and the minimum prey density in the last 500 time steps is plotted on a log scale.

74

oscillations, as we have shown analytically, need not result in a significantly higher risk of extinction (i.e. the minimum population densities are significantly higher than Ñ). Moreover, more freely moving enemies appear to always increase the minimum population densities and decrease the amplitudes of the population oscillations.

Adding victim density-dependence

Thus far density dependence has only manifested itself in these models via the enemy's functional and numerical response. The inclusion of victim density dependence tends to have a stabilizing effect on thesource dynamics. To illustrate how victim density–dependence influences our earlier results, we include it in the victimless sink model with ideal-free movement:

$$\frac{dN}{dt} = \begin{cases} r\,N(1-N/K) & \text{if } r_2 > h(N) \\ r\,N(1-N/K) - P\,N\,g(N) & \text{if } r_2 < h(N) \end{cases}$$

$$\frac{dP}{dt} = \begin{cases} -r_2\,P & \text{if } r_2 > h(N) \\ P\,h(N) & \text{if } r_2 < h(N) \end{cases} \tag{6}$$

where K is the carrying capacity of the victim. Since the victim numerical response was not changed, the switching line is still given by $N = h^{-1}(r_2)$. The behaviors of population trajectories hitting the switching line are similar to the solutions for (5) (Fig. 4). The inclusion of this victimless sink has a long-term effect only if there is a periodic trajectory for (6) whose minimum victim density is less than $h^{-1}(r_2)$ (Fig. 8a). This occurs, for instance, if the system is sufficiently enriched (i.e. K is sufficiently large), or the enemy nullcline $N = h^{-1}(0)$ is sufficiently close to the enemy axis. In these cases, the inclusion of the victimless sink strongly dampens the amplitude of the enemy–victim oscillations (Fig. 8b).

Discussion

Models, experiments, and field studies have shown that enemy-victim interactions in homogenous environments can exhibit boom and bust cycles that result in the extinction of one or both species (Utida 1957, Huffaker 1958, Luckinbill 1973, Murdoch and Oaten 1975, Hassell 1978). We prove that this can occur for victim-enemy models with a saturating enemy functional response and density-independent victim dynamics. Spatial or population heterogeneity can stabilize these unbounded oscillations (Hassell 1978, Sabelis et al. 1991, van Baalen and Sabelis 1993, Schreiber et al. 2000) even when the heterogeneity is generated by sink habitats; habitats in which a species' death rate exceeds its birth rate. For example, Holt (1985) showed that passive dispersal of the enemy into a victimless habitat or state (a sink for the enemy) can stabilize the enemy-victim equilibrium. This equilibrium, however, is not evolutionarily stable as individuals avoiding the victimless sink maintain a higher per-capita growth rate. To understand how evolutionarily stable sink populations arise, we analyzed enemy-victim dynamics in which one species moves in an ideal–free manner in and out of a sink (see Cressman et al. 2004 for a discussion about the relationship between ideal–free distributions and evolutionarily stable strategies). According to Holt (1985, p. 196) "the ultimate effect of this on population size and stability is not at all obvious." Our analysis proves that the ideal-free movement into a sink promotes persistence by shifting the dynamics from undamped oscillations to a globally stable periodic motion. Along this periodic motion, the ideal-free species moves in and out of the sink, thereby maintaining an ecologically persistent and evolutionarily stable sink population. Moreover, we prove that the longer the sink can sustain a population, the smaller the amplitude of the enemy-victim oscillations and the higher the minimum victim density. These results apply both to enemy-free sinks and victimless sinks.
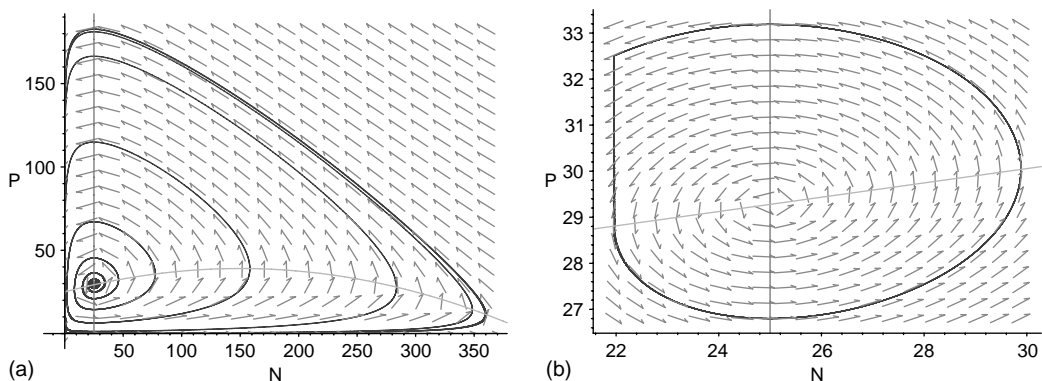
Fig. 8. In (a), a phase portrait of (6) with victim and enemy densities on the horizontal and vertical axes, respectively. In (b), the effect of including a victimless sink.

Our results for ideal-free movement are related to four earlier studies (Křivan 1997, 1998, van Baalen and Sabelis 1999, Bernstein et al. 1999). Křivan (1997) considered a two-patch model in which each patch had a classical Lotka-Volterra enemy–victim interaction with a neutrally stable equilibrium. This classical interaction does not permit persistence as arbitrarily low levels of demographic or environmental stochasticity result in irregular undamped oscillations resulting in the extinction of one or both species. Křivan proved that ideal-free movement between the patches results in a global attractor consisting of a neutrally stable equilibrium surrounded by periodic motions. Křivan found similar results for a two patch model where one of the patches acted as a refuge for the prey. While ideal-free movement promotes persistence in both of these models, the inclusion of arbitrarily low levels of noise into these models will result in bounded irregular oscillations with no well-defined amplitude or period. Our analysis highlights this structural instability. We prove that predator satiation (no matter how slight) in conjunction with ideal-free movement results in a globally stable periodic-motion which is structurally stable (Broucke et al. 2001). In particular, these oscillations have well-defined amplitudes and periods even in the presence of small random perturbations. Bernstein et al. (1999) analyzed a continuous-time enemy-victim interaction with three source patches frequented by all species and with a type II functional response accounting for interference. When both species disperse rapidly and the victim disperses passively, Bernstein et al. proved that optimal foraging of the enemy has no effect on the stability as the patches effectively merge into one patch. van Baalen and Sabelis (1999) considered multi-patch enemy-victim interactions in which each patch exhibited Nicholson-Bailey dynamics. These models assume the species have synchronized generations and within a patch generate undamped oscillations. When both species exhibit ideal-free movement, simulations of the interactions yield either extinction or coexistence via chaotic fluctuations. Unlike our results, periodic or equilibrium coexistence was not observed. The inclusion of sink patches resulted in less extreme albeit chaotic fluctuations and promoted persistence. As proposed by Holt (1997), these fluctuations in population densities, whether periodic or aperiodic, generate moments in time where fitness in the sinks exceeds fitness in the sources. During these moments, ideal-free populations move into the sinks and create evolutionarily stable and ecologically persistent sink populations.

Due to constraints on dispersal, information gathering, or learning, individuals may make sub-optimal decisions about patch selection (Holt 1997, van Baalen and Sabelis 1993, Bernstein et al. 1999, Bolker et al. 2003). Our simulations illustrate that these constraints have significant effects on the stability and persistence of

enemy-victim interactions. Moreover, these effects depend critically on which species disperses. When dispersing in and out of enemy-free sinks, victims that respond more ideally to the spatial variation in fitness tend to dampen population oscillations without having a substantial impact on the mean population abundance. In contrast, when dispersing in and out of victimless sinks, enemies that respond more ideally to the spatial variation in fitness can lower mean population abundance and amplify population oscillations. Using their three patch model, Bernstein et al. (1999) also considered the effect of sub-optimal behavior of the enemy on stability. They assumed that enemies, for a fraction e of time, make optimal decisions and disperse randomly otherwise. They found that the amount of predator interference required for stability was minimized at intermediate values of e. Hence, depending on the nature of the ecological and environmental details, suboptimal behavior can stabilize or destabilize species interactions.

Empirical evidence

An enemy-free sink is a state in which the victims have little or no chance of encountering natural enemies and in which the victims per-capita growth rate is negative. Spatial refugia for victims can form enemy-free sinks. For example, rock crevices may provide limited access to sea otters foraging on abalones in central California (Hines and Pearse 1982). Some abalones (including *Haliotis kamtschatkana*) feed primarily on diatoms and small algae (Paul et al. 1977) that cannot grow well in shaded crevices. Though crevice populations have remained stable at 1.8 abalones 10 m^{-2} over the time period of intense sea otter predation 1972–1981 (indicating constant survivorship and recruitment rates; Hines and Pearse 1982), transport via the California Current may have provided recruitment to crevice populations from abalone populations further north, outside of the range of sea otters. Thus, we postulate that these crevice populations represent enemy-free sinks that require larvae from outside (i.e. source) populations to persist. Alternatively, *Tegula* snails have a spatial refuge from sea star predation in kelp plants and off the bottom where sea stars forage (Watanabe 1984). These habitats may be sub-optimal and form enemy-free sinks, as snails prefer residence on the kelp forest floor in shallower depths where predators are absent. Enemy-free sinks are likely to be common in ecosystems degraded by anthropogenic stress (Jackson et al. 2001). For instance, eutrophication has caused many freshwater and marine habitats to have greatly reduced levels of dissolved oxygen (i.e. hypoxia) (Diaz and Rosenberg 1995, Rabalais and Turner 2001). In freshwater systems, yellow perch (*Perca flavescens*) has a lower tolerance for hypoxic habitats than one of its prey species, fathead

76

minnow (*Pimephales promelas*). Hypoxic environments that are lethal to perch, but not to fathead minnows, could provide enemy-free refuges (Robb and Abrahams 2002). In estuarine and marine habitats that experience periodic hypoxia, the Baltic clam (*Macoma balthica*) is able to persist, but a major predator of Baltic clams, the blue crab, *Callinectes sapidus*, is unable to forage effectively (Seitz et al. 2003) and typically emigrates from these habitats (Pihl et al. 1991, 1992). Since the victim species persists in hypoxic habitats under physiologically stressful conditions where growth and reproduction are impaired (Seitz et al. 2003), these examples may be enemy-free sinks. Terrestrial systems have similar examples of enemy-free or victimless sinks. For instance, voles migrate from meadows or fields (which are optimal habitats) to bogs (which are 'sub-optimal' habitats) during periods of high vole abundance, and predator foraging efficiency is decreased in those bog habitats (i.e. enemy-free sinks). Surviving vole sub-populations in the bogs can re-colonize field habitats after predation has reduced the vole populations there. This movement between sources and sinks by the prey leads to population stabilization. Planthoppers (Hemiptera: Delphacidae) and their suite of predators and parasitoids show a similar trend. A meta-analysis by Denno and Peterson (2000) indicates that highly mobile species of planthoppers that can move from one patch of habitat to another in response to high predator pressure tend to have stable populations, whereas those that are less mobile tend to exhibit frequent population outbreaks followed by crashes. Thus, the movement between habitats that vary in quality and predation pressure leads to stability in the system.

Our analysis proves that ideal-free movement by the victim into the enemy-free sink can result in a globally stable periodic motion. Along this periodic motion, victims enter the sink when enemy densities are high and leave the sink when enemy densities are low. This type of victim movement has been observed in natural populations although the victim response to enemy density is confounded with seasonal and daily fluctuations of environmental cues. For instance, a study on caribou populations (Bergerud 1988) showed that caribou herds that moved out of comparatively rich forested lands to sparsely vegetated tundra during times of increased predation risk from wolves exhibited higher levels of population growth than did herds that stayed in the forest. Although the herds did not appear to live permanently in the tundra habitat because of food limitation, this habitat seemed to be necessary for a herd to thrive. Indeed, many of the herds that did not migrate declined because of the wolf predation, thus showing the potential importance of sink habitats as a temporary refuge. Another natural situation involves diel vertical migration of zooplankton in lakes and marine ecosystems (Neill 1990, Bollens and Frost 1991). At night, predatory zooplankton migrate up in the water column where they can feed on phytoplankton and small zooplankton, but where their visually-hunting predators (e.g. fish, diving birds) are unable to forage successfully. During daytime, the predatory zooplankton migrate deep out of the photic zone where they can avoid visually hunting predators, but where there is low food availability, thereby creating a temporal enemy-free sink for the predatory zooplankton.

A victimless sink (or victimless space) is a state in which the enemy has limited or no access to victims. One instance of victimless sinks involves changes in the functional response of predators due to changes in prey density. Planktonic filter-feeding invertebrates, such as copepod crustaceans, increase the proportion consumed of available prey as prey density declines. However, at a threshold of low prey density, feeding ceases in some species of copepods (Porter et al. 1984), thus creating a behavioral victimless sink. Another instance of victimless sinks arises due to movement of the enemy through spatially heterogenous landscapes. For example, the prey landscape for the blue crab is composed of prey patches (e.g. Baltic clam) on the order of 10–100 m (Hines et al. 1995, Seitz and Lipcius 2001). The surrounding matrix is free of suitable prey, but must be traversed by foraging crabs moving between prey patches (Hines et al. 1995). Moreover, within any particular prey patch, crabs are antagonistic such that mutual interference reduces crab foraging efficiency (Mansour and Lipcius 1991, Clark et al. 1999a, 1999b), leading some crabs to emigrate to different prey patches. Hence, the prey landscape for the blue crab comprises (1) source habitats where prey are available but where aggressive interactions can become so intense as to cause some crabs to depart, and (2) victimless sinks where prey are lacking but which must be negotiated to reach alternative prey patches. In a terrestrial example of a victimless sink, eastern coyotes (*Canis latrans*) in Canadian forest systems switch from feeding primarily on small animals to feeding on berries during the summer (Tremblay et al. 1998). This switch in feeding behavior was correlated with lower body size and lower pup survival as compared to populations where consumption of animal flesh was the primary source of food year round. This is an example of a behavior-mediated victimless sink, as the coyotes do not leave the forest habitats but rather stop hunting their preferred prey.

Implications for conservation and management

In applied population ecology these results are relevant in at least three areas – fisheries ecology and management (Quinn and Deriso 1999), pest control (Berryman 1999), and conservation and restoration biology (Burgman et al. 1993). For instance, in fisheries management

and marine biodiversity conservation, there is a worldwide focus on the implementation of marine reserve networks, with emphasis on the protection of source habitats (Crowder et al. 2000, Lipcius et al. 2001), while sink habitats are deemed too poor to be worth protecting. Moreover, there is a general opposition to the protection of sink habitats, reasoning that protection of sinks takes away from the metapopulation by redirection of conservation activities away from source habitats. Similarly, in pest control, one logical strategy is to eradicate or reduce pests in source habitats, reasoning that elimination of source populations will lead to the demise of the metapopulation (Berryman 1999). This study demonstrates that sink habitats warrant serious consideration in conservation and management. Since a sink habitat may stabilize enemy–victim interactions, the destruction of 'poor quality' habitats could result in the crash of the population, whether for good in the case of pests, or for bad in the case of populations needing restoration or conservation. Similarly, Jonzen et al. (2005) demonstrate that trend detection in metapopulations may be more effectively achieved by monitoring populations in sink rather than source habitats, under a diverse set of environmental and demographic conditions. It is becoming clear that a sound understanding of source–sink dynamics, especially for multi-species interactions, is critical in making correct conservation and management decisions.

References

Bergerud, A. T. 1988. Caribou, wolves and man. – Trends Ecol. Evol. 3: 68–72.

Bernstein, C., Auger, P. and Poggiale, J. C. 1999. Predator migration decisions, the ideal free distribution, and predator-prey dynamics. – Am. Nat. 153: 267–281.

Berryman, A. A. 1999. The theoretical foundations of biological control. – In: Hawkins, B. A. and Cornell, H. V. (eds), Theoretical approaches to biological control. Cambridge Univ. Press, pp. 1–21.

Bolker, B., Holyoak, M., Křivan, V. et al. 2003. Connecting theoretical and empirical studies of trait-mediated interactions. – Ecology 84: 1101–1114.

Bollens, S. M. and Frost, B. W. 1991. Diel vertical migration in zooplankton: rapid individual response to predators. – J. Plankton Res. 13: 1359–1365.

Broucke, M., Pugh, C. C. and Simic, S. 2001. Structural stability of piecewise smooth systems. – Comput. Appl. Math. 20: 51–90.

Burgman, M. A., Ferson, S. and Akcakaya, H. R. 1993. Risk assessment in conservation biology. – Chapman and Hall.

Clark, M. E., Wolcott, T. G., Wolcott, D. L. et al. 1999a. Foraging and agonistic activity co-occur in free-ranging blue crabs (Callinectes sapidus): observation of animals by ultrasonic telemetry. – J. Exp. Mar. Biol. Ecol. 233: 143–160.

Clark, M. E., Wolcott, T. G., Wolcott, D. L. et al. 1999b. Intraspecific interference among foraging blue crabs Callinectes sapidus: interactive effects of predator density and prey patch distribution. – Mar. Ecol. Prog. Ser. 178: 69–78.

Cressman, R., Krivan, V. and Garay, J. 2004. Ideal free distributions, evolutionary games, and population dynamics in multiple-species environments. – Am. Nat. 164: 473–489.

Crowder, L. B., Lyman, S. J., Figueira, W. F. et al. 2000. Source-sink population dynamics and the problem of siting marine reserves. – Bull. Mar. Sci. 66: 799–820.

Denno, R. F. and Peterson, M. A. 2000. Caught between the devil and the deep blue sea, mobile planthoppers elude natural enemies and deteriorating host plants. – Am. Entomol. 46: 95–109.

Dias, P. C. 1996. Sources and sinks in population biology, Trends Ecol. Evol. 11: 326–330.

Diaz, R. J. and Rosenberg, R. 1995. Marine benthic hypoxia: a review of its ecological effects and the behavioural responses of benthic macrofauna. – Oceanogr. Mar. Biol. Annu. Rev. 33: 245–303.

Goh, B. S. 1980. Management and analysis of biological populations. – Elsevier.

Hassell, M. P. 1978. The dynamics of arthropod predator-prey systems. – Monogr. Popul. Biol., vol. 13, Princeton Univ. Press.

Hines, A. H. and Pearse, J. S. 1982. Abalones, shells and sea otters: dynamics of prey populations in central California. – Ecology 63: 1547–1560.

Hines, A. H., Wolcott, T. G., Gonzalez-Gurriaran, E. et al. 1995. Movement patterns and migrations in crabs: telemetry of juvenile and adult behaviour in Callinectes sapidus and Maja squinado. – J. Mar. Biol. Ass. UK 75: 27–42.

Holt, R. D. 1984. Spatial heterogeneity, indirect interactions, and the coexistence of prey species. – Am. Nat. 124: 377–406.

Holt, R. D. 1985. Population dynamics in two patch environments: some anomalous consequences of optimal habitat distribution. – Theor. Popul. Biol. 28: 181–208.

Holt, R. D. 1997. On the evolutionary stability of sink populations. – Evol. Ecol. 11: 723–731.

Huffaker, C. B. 1958. Experimental studies on predation: dispersion factors and predator-prey oscillations. – Hilgardia 27: 343–383.

Jackson, J. B. C., Kirby, M. X., Berger, W. H. et al. 2001. Historical overfishing and the recent collapse of coastal ecosystems. – Science 293: 629–638.

Jeffries, M. J. and Lawton, J. H. 1984. Enemy-free space and the structure of ecological communities. – Biol. J. Linn. Soc. 23: 269–286.

Jonzen, N., Rhodes, J. R. and Possingham, H. P. 2005. Trend detection in source-sink systems: when should sink habitats be monitored? – Ecol. Appl. 15: 326–334.

Křivan, V. 1997. Dynamic ideal free distribution: effects of optimal patch choice on predator-prey dynamics. – Am. Nat. 149: 164–178.

Křivan, V. 1998. Effects of optimal antipredator behavior of prey on predator-prey dynamics: role of refuges. – Theor. Popul. Biol. 53: 131–142.

Lawton, J. H. and McNeill, S. 1979. Between the devil and the deep blue sea: on the problem of being an herbivore. – Symp. Br. Ecol. Soc. 20: 223–244.

Lipcius, R. N., Stockhausen, W. T. and Eggleston, D. B. 2001. Marine reserves for Caribbean spiny lobster: empirical evaluation and theoretical metapopulation dynamics. – Mar. Freshwater Res. 52: 1589–1598.

Luckinbill, L. S. 1973. Coexistence in laboratory populations of Paramecium aurelia and its predator Didinium nasutum. – Ecology 54: 1320–1327.

Mansour, R. A. and Lipcius, R. N. 1991. Density-dependent foraging and mutual interference in blue crabs preying upon infaunal clams. – Mar. Ecol. Prog. Ser. 72: 239–246.

May, R. M. 1981. Theoretical ecology: principles and application. – Sinauer Ass.

McNair, J. N. 1986. The effects of refuges on predator-prey interactions: a reconsideration. – Theor. Popul. Biol. 29: 38–63.

McNair, J. N. 1987. Stability effects of prey refuges with entry-exit dynamics. – J. Theor. Biol. 125: 449–464.

Murdoch, W. W. and Oaten, A. 1975. Predation and population stability. – Adv. Ecol. Res. 9: 2–131.

Neill, W. E. 1990. Induced vertical migration in copepods as a defense against invertebrate predation. – Nature 345: 524–526.

Paul, A., Paul, J., Hood, D. et al. 1977. Observations on food preferences, daily ration requirements and growth of *Haliotis kamtschatkana* Jonas in captivity. – Veliger 19: 303–309.

Pihl, L., Baden, S. P. and Diaz, R. J. 1991. Effects of periodic hypoxia on distribution of demersal fish and crustaceans. – Mar. Biol. 108: 349–360.

Pihl, L., Baden, S. P., Diaz, R. J. et al. 1992. Hypoxia-induced structural changes in the diet of bottom feeding fish and crustacea. – Mar. Biol. 112: 349–361.

Porter, K. G., Orcutt, J. D. Jr. and J. Gerritsen. 1983. Functional response and fitness in a generalist filter feeder, *Daphnia magna* (Cladocera: Crustacea). – Ecology 64: 735–742.

Pulliam, H. R. 1988. Sources, sinks, and population regulation. – Am. Nat. 132: 652–661.

Quinn, T. J. and Deriso, R. B. 1999. Quantitative fish dynamics. – Oxford Univ. Press.

Rabalais, N. N. and Turner, R. E. (eds). 2001. Coastal hypoxia. Consequences for living resources and ecosystems. – Coastal Estuarine Studies Vol. 58. Am. Geophys. Union, Washington, DC.

Robb, T. and Abrahams, M. V. 2002. The influence of hypoxia on risk of predation and habitat choice by fathead minnow, *Pimephales promelas*. – Behav. Ecol. Sociobio. 52: 25–30.

Sabelis, M. W., Diekmann, O. and Jansen, V. A. A. 1991. Metapopulation persistence despite local extinction: predator-prey patch models of the Lotka-Volterra type. – Biol. J. Linn. Soc. 42: 267–283.

Schreiber, S. J., Fox, L. R. and Getz, W. M. 2000. Coevolution of contrary choices in host-parasitoid systems. – Am. Nat. 155: 637–648.

Seitz, R. D. and Lipcius, R. N. 2001. Variation in top-down and bottom-up control of marine bivalves at differing spatial scales. – ICES J. Mar. Sci. 58: 689–699.

Seitz, R. D., Marshall, L. S., Hines, A. H. et al. 2003. Effects of hypoxia on the Baltic clam (*Macoma balthica*) and predation by the blue crab (*Callinectes sapidus*) in Chesapeake Bay. – Mar. Ecol. Progr. Ser. 257: 179–188.

Tremblay, J.-P., Crête, M. and Huot, J. 1998. Summer foraging behavior of eastern coyotes in rural versus forest landscape: a possible mechanism of source-sink dynamics. – Ecoscience 5: 172–182.

Utida, S. 1957. Population fluctuation, an experimental and theoretical approach. – Cold Spring Harbor Symp. Quant. Biol. 22: 139–1151.

van Baalen, M. and Sabelis, M. W. 1993. Coevolution of patch selection strategies of predator and prey and the consequences for ecological stability. – Am. Nat. 142: 646–670.

van Baalen, M. and Sabelis, M. W. 1999. Nonequilibrium population dynamics of ''ideal and free'' prey and predators. – Am. Nat. 154: 69–88.

Watanabe, J. M. 1984. The influence of recruitment, competition, and benthic predation on spatial distributions of three species of kelp forest gastropods (Trochidae: Tegula). – Ecology 65: 920–936.

Ylönen, H., Pech, R. and Davis, S. 2003. Heterogeneous landscapes and the role of refuge on the population dynamics of a specialist predator and its prey. – Evol. Ecol. 17: 349–369.

Subject Editor: Tim Benton

Appendix A. The unbounded dynamics of (1)

Consider the following model where N is the victim density, P the enemy density, r is the intrinsic rate of growth of the victim, Ng(N) is the enemy functional response, and h(N) is the numerical response of the enemies

$$\frac{dN}{dt} = r\,N - N\,P\,g(N) \tag{7}$$

$$\frac{dP}{dt} = P\,h(N)$$

As stated earlier, we assume that Ng(N) is increasing, g(N) is decreasing, and h(N) is increasing and saturating. Provided that $\rho = \lim_{N \to \infty} h(N) > 0$, this system has a unique positive equilibrium, $(N^*, P^*) = (h^{-1}(0), \frac{r}{g(N^*)})$.

Linearization about the positive equilibrium (N^*, P^*) gives

$$\begin{bmatrix} -N^*\,P^*g'(N^*) & -N^*\,g(N^*) \\ P^*h'(N^*) & 0 \end{bmatrix}$$

Since $g'(N^*) < 0$, the trace and determinant of this matrix is positive and (N^*, P^*) is unstable. Consider the change of variables $u = \ln(N)$ and $v = \ln(P)$ on the positive quadrant. With respect to this change of coordinates, (7) becomes

$$\frac{du}{dt} = r - e^v\,g(e^u) \tag{8}$$

$$\frac{dv}{dt} = h(e^u)$$

The divergence of (8) is given by $-e^v g'(e^u)e^u$. As g is a decreasing function, the divergence is always positive. Hence, by the Bendixson criterion, there are no periodic orbits in the positive quadrant. Poincaré-Bendixson theory implies that any bounded solution must contain equilibria in its ω-limit set. As the two equilibria in the

non-negative quadrant are unstable, the only bounded solutions in the non-negative quadrant are the equilibria.

Now suppose that $\rho > r$. We will show that the solutions exhibit unbounded oscillations. The nontrivial N and P nullclines divide the positive quadrant into four distinct regions: I where $\frac{dN}{dt} > 0$ and $\frac{dP}{dt} > 0$, II where $\frac{dN}{dt} < 0$ and $\frac{dP}{dt} > 0$, III where $\frac{dN}{dt} < 0$ and $\frac{dP}{dt} < 0$, and IV where $\frac{dN}{dt} > 0$ and $\frac{dP}{dt} < 0$. We begin by showing a non-equilibrium solution $(N(t), P(t))$ with $N(0) > 0$ and $P(0) > 0$ can not remain in region I for all $t \geq 0$. Suppose to the contrary the solution remains in region I for all $t \geq 0$. Let $\epsilon = \frac{\rho - r}{2}$. As $\frac{dN}{dt} > 0$ and $\frac{dP}{dt} > 0$ in region I, $N(t)$ and $P(t)$ are increasing without bound. Hence, there exists $T > 0$ such that $h(N(t)) \geq \rho - \epsilon$ for $t \geq T$. It follows that

$$P'(t) \geq (\rho - \epsilon)P(t)$$

for $t \geq T$. Therefore, $P(t) \geq P(T)e^{(\rho - \epsilon)(t - T)}$ for $t \geq T$. Setting $s = N(T)g(N(T)) > 0$, we get that

$$N'(t) \leq r\,N(t) - s\,P(T)e^{(\rho - \epsilon)(t - T)}$$

for $t \geq T$. This differential inequality implies

$$N(t) \leq \left(N(T) + \frac{s\,P(T)}{\rho - r - \epsilon}\right)e^{r(t - T)}$$
$$- \frac{s\,P(T)}{\rho - r - \epsilon}e^{(\rho - \epsilon)(t - T)}$$

for $t \geq T$. However as $\rho - \epsilon > r$, we get that $N(t) < 0$ for t sufficiently large which is absurd! Hence, any solution entering region I must eventually leave region I. As $N(t)$ and $P(t)$ are increasing in region I, a solution leaving region I must enter region II. The definitions of the regions, the fact that the non-zero N nullcline (i.e. $P = \frac{r}{g(N)}$) is an increasing function of N, and the non-zero P nullcline is a vertical line imply any solution entering region II must leave region II and enter region III, any solution entering region III must leave region III and enter region IV, and any solution entering region IV must leave region IV and enter region I. Combining these results imply that any non-equilibrium solution cycles indefinitely in forward time through regions I, II, III, and IV. Let $\Gamma_1 = \{(h^{-1}(0), P): 0 \leq P \leq P^*\}$ i.e. the lower half of the vertical P nullcline. By Poincaré-Bendixson theory, the instability of the positive equilibrium and the lack of periodic solutions, any non-equilibrium solution in forward time intersects Γ_1 in a decreasing sequence of points that converges to $(h^{-1}(0), 0)$. Let $\Gamma_2 = \{(h^{-1}(0), P): P^* \leq P\}$ i.e. the upper half of the vertical P nullcline. By Poincaré-Bendixson theory and instability of the positive equilibrium, any non-equilibrium solution in forward time intersects Γ_2 in an increasing sequence of points that converges to

$(h^{-1}(0), \infty)$. Hence, any non-equilibrium solution in forward time comes arbitrarily close to the N and P axes.

The previous arguments imply (in general) any positive non-equilibrium solution $(N(t), P(t))$ either oscillates between regions I, II, III, and IV, or there is a $T > 0$ such that $(N(t), P(t))$ lies in region I for $t \geq T$. In the first case, the limit set of $(N(t), P(t))$ is the N and P axes. In the later case $\lim_{t \to \infty} N(t) = \lim_{t \to \infty} P(t) = +\infty$. Suppose that $r > \rho$. We will show that every positive non-equilibirium solution $(N(t), P(t))$ satisfies $\lim_{t \to \infty} N(t) = \lim_{t \to \infty} P(t) = +\infty$ by contradiction. Define $\sigma = \lim_{N \to \infty} N\,g(N)$. Assume to the contrary that the solution oscillates between regions I, II, III, and IV. It follows that limit set of $(N(t), P(t))$ contains the N-axis. Hence, there exists $T \geq 0$ such that $N(T) > \frac{2}{r - \rho}\frac{\sigma P(T)}{}$. Since $h(N) \leq \rho$ for all $N > 0$, $\rho P(t) \geq h(N(t))\,P(t) = P'(t)$ for $t \geq 0$. Thus, $P(t)e^{\rho(t-T)} \geq P(t)$ for all $t \geq T$. On the other hand, $N'(t) \geq r\,N(t) - \sigma P(T)e^{\rho(t-T)}$ for all $t \geq T$. This differential inequality and our choice of T imply

$$N(t) \geq \left(N(T) - \frac{\sigma\,P(T)}{r - \rho}\right)e^{r(t - T)} + \frac{\sigma\,P(T)}{r - \rho}e^{\rho(t - T)}$$
$$\geq \frac{\sigma\,P(T)}{r - \rho}e^{r(t - T)} + \frac{\sigma\,P(T)}{r - \rho}e^{\rho(t - T)}$$

for all $t \geq T$. Since $r > \rho$, $\lim_{t \to \infty} N(t) = \infty$. Since $\rho = \lim_{N \to \infty} h(N) > 0$, there exists $\tau > 0$ such that $h(N(t)) > \rho/2$ for all $t \geq \tau$. Since $P'(t) \geq P(t)\rho/2$ for $t \geq \tau$, $P(t) \geq P(\tau)e^{\rho(t - \tau)/2}$ for all $t \geq \tau$ and $\lim_{t \to \infty} P(t) = \infty$.

Appendix B. The dynamics of (4)

When a population trajectory slides along the switching curve, there is an unique α that determines the convex combination of the growth rate vectors lying immediately above and below the switching curve that yields a vector tangent to the switching curve. More precisely, α satisfies

$$-\frac{r - r_2}{g(N)^2}g'(N) = \frac{P\,\alpha\,h(N) + P\,(1 - \alpha)\,h(0)}{r\alpha N - \alpha NPg(N) + r_2(1 - \alpha)N} \quad (9)$$

where the left hand side is the slope of the switching curve and the right hand side is the slope of the growth rate vector along the switching curve.

To understand the global dynamics of (4), we make three observations about population trajectories near the switching curve. First, the switching curve $P = \frac{r - r_2}{g(N)}$ is an increasing function of N. Second, to the right of the enemy-nullcline, the enemy growth rate is positive below the switching curve and negative above the switching curve. Consequently, population trajectories that hit the switching curve to the right of the enemy nullcline slide down the switching curve to the left of the enemy nullcline. Third, at $N = 0$ the enemy growth rate is

negative above and below the switching curve. Consequently, population trajectories hitting the switching curve near $N = 0$ pass through the switching curve. These three observations imply there is a positive victim density $\hat{N} < N^*$ such that population trajectories hitting the switching curve to the right of $\hat{N}$ slide down the switching curve until reaching $\hat{N}$. After reaching $\hat{N}$, the population trajectory enters the region below the switching curve. For example, consider a type II functional response $Ng(N) = \frac{a\,N}{1 + T_h a\,N}$ and the associated numerical response $h(N) = \theta\,N\,g(N) - m$ where a, T_h, θ, and m are the enemy's searching efficiency, handling time, conversion efficiency, and per-capita mortality rate. For these equations the switching curve is the line $P = (r - r_2)(1/a + T_h N)$ and the critical victim density is $\hat{N} = \frac{m}{T_h\,a(\rho - r_2)}$.

These previous observations show how a population trajectory moving along the switching curve generates a periodic trajectory. Consider a solution $(N(t), P(t))$ of (4) initiated at $(\hat{N}, (r - r_2)/g(\hat{N}))$. This solution will initially move below the switching curve and move to the right of the enemy nullcline. If this trajectory hits the switching curve to the right of the enemy nullcline, then the population trajectory slides down the switching curve until $(\hat{N}, (r - r_2)/g(\hat{N}))$ thereby creating a periodic trajectory. When such a periodic trajectory exists, all solutions that hit the sliding curve to the right of the enemy nullcline eventually follow this periodic trajec-tory. To see when this periodic trajectory exists. Notice that below the switching curve, (1) and (5) are equivalent. Since (1) exhibits unbounded oscillations when $\rho > r$ (i.e. (1) is an enemy-victim sink), all positive trajectories of (5) eventually hit the switching curve. Hence, when $\rho > r$, there is a unique periodic trajectory that attracts all positive non-equilibrium trajectories. The value of α along the periodic orbit is 1 off of the switching curve and given by (9) on the switching curve.

Appendix C. The dynamics of (6)

In this Appendix, we determine an explicit expression for α along the switching line. This α determines the unique convex combination of the growth rate vectors on either side of the switching line that is tangent to the switching line. More precisely, since the switching line is vertical, α must satisfy

$$0 = \alpha(r\,N - N\,P\,g(N)) + (1 - \alpha)r\,N$$

Since $N = h^{-1}(r_2)$ on the switching line, α is given by

$$\alpha = \frac{r}{P g(h^{-1}(r_2))}$$

whenever $P > \frac{r}{g(h^{-1}(r_2))}$.